Analysis of a Thick Dichroic Plate with Rectangular Holes at Arbitrary Angles of Incidence

J. C. Chen
Ground Antennas and Facilities Engineering Section

A thick dichroic plate that is transparent to one frequency band while at the same time reflective to other frequencies is needed for high-power transmission in the Deep Space Network. Software based on the method of moments was developed to design a thick dichroic plate with rectangular holes. A test dichroic plate was fabricated, and an experiment was performed to verify the computer code. Good agreement was found between theory and experiment.

I. Introduction

The Deep Space Network has a need for dichroic plates having an insertion loss as low as 0.04 dB at the passband and the ability to handle up to 500 kW of power [1]. Because a thin dichroic plate may not be mechanically suitable for these requirements, a thick dichroic plate design is considered. Also, using rectangular rather than circular holes provides the designer with an extra degree of freedom. Therefore a study of a thick dichroic plate with rectangular holes was made, and a computer code was developed.

The relationship between the rectangular holes, the array lattice of an infinite dichroic plate, and the incident wave is shown in Fig. 1. The design variables of the software are hole size, lattice size and shape, thickness of the plate, dielectric constant in the hole, and angle of incidence of the linearly polarized wave. The program calculates the amplitude and phase of both the transmission and reflection coefficients of the two orthogonal linear polarizations (TE and TM). The program was run on JPL's Cray X-MP/18 supercomputer.

II. Analysis

The analysis of a thick dichroic plate with rectangular holes is carried out in a series of steps. First, a model of a half-space infinite array is constructed. A complete set of basis functions with unknown coefficients is developed for the waveguide region (waveguide modes) and for the free-space region (Floquet modes) in order to represent the electromagnetic fields [2]. Next, the boundary conditions are applied at the interface between these two regions. The method of moments is used to compute the unknown mode coefficients [3,4]. The scattering matrix of the half-space infinite array is then calculated. The reference plane of the scattering matrix is moved half a plate thickness in the negative z direction. Finally, a dichroic plate of finite thickness is synthesized by positioning two plates of half thickness back to back. The total scattering matrix is

obtained by cascading the scattering matrices of the two half-space infinite arrays.

A. Floquet Modes and Waveguide Modes

The analysis starts with an infinite array in half space, Fig. 2(a), consisting of a free-space region ($z > 0$) and a waveguide region ($z < 0$). The electromagnetic fields in each region are represented by a set of orthonormal basis functions, Floquet and waveguide modes respectively, which satisfy Maxwell's equations. The Floquet modes are given by

$$\overline{\Psi}^{TE}_{mn}(x,y) = \frac{1}{\sqrt{D_x D_y \sin\Omega}} \frac{\beta_n \hat{x} - \alpha_m \hat{y}}{\sqrt{\alpha_m^2 + \beta_n^2}} e^{j(\alpha_m x + \beta_n y)} \quad (1)$$

for Floquet TE_{mn} modes, and

$$\overline{\Psi}^{TM}_{mn}(x,y) = \frac{1}{\sqrt{D_x D_y \sin\Omega}} \frac{\alpha_m \hat{x} + \beta_n \hat{y}}{\sqrt{\alpha_m^2 + \beta_n^2}} e^{j(\alpha_m x + \beta_n y)} \quad (2)$$

for Floquet TM_{mn} modes, with

$$\alpha_m = \frac{2\pi m}{D_x} - k_0 \sin\theta \cos\phi \quad (3)$$

and

$$\beta_n = \frac{2\pi n}{D_y \sin\Omega} - \frac{2\pi m}{D_x} \cot\Omega - k_0 \sin\theta \sin\phi \quad (4)$$

where k_0 is the wave number in the free space.

The waveguide modes are given by

$$\overline{\Phi}^{TE}_{mn}(x,y) = \frac{1}{\sqrt{\left(\frac{m\pi}{H_x}\right)^2 + \left(\frac{n\pi}{H_y}\right)^2}} \sqrt{\frac{\epsilon_m \epsilon_n}{H_x H_y}}$$

$$\times \left[\frac{n\pi}{H_y} \cos\left(\frac{m\pi x}{H_x} + \frac{m\pi}{2}\right) \sin\left(\frac{n\pi y}{H_y} + \frac{n\pi}{2}\right) \hat{x} \right.$$

$$\left. - \frac{m\pi}{H_x} \sin\left(\frac{m\pi x}{H_x} + \frac{m\pi}{2}\right) \cos\left(\frac{n\pi y}{H_y} + \frac{n\pi}{2}\right) \hat{y} \right] \quad (5)$$

for rectangular waveguide TE_{mn} modes, and

$$\overline{\Phi}^{TM}_{mn}(x,y) = \frac{1}{\sqrt{\left(\frac{m\pi}{H_x}\right)^2 + \left(\frac{n\pi}{H_y}\right)^2}} \sqrt{\frac{\epsilon_m \epsilon_n}{H_x H_y}}$$

$$\times \left[\frac{m\pi}{H_x} \cos\left(\frac{m\pi x}{H_x} + \frac{m\pi}{2}\right) \sin\left(\frac{n\pi y}{H_y} + \frac{n\pi}{2}\right) \hat{x} \right.$$

$$\left. + \frac{n\pi}{H_y} \sin\left(\frac{m\pi x}{H_x} + \frac{m\pi}{2}\right) \cos\left(\frac{n\pi y}{H_y} + \frac{n\pi}{2}\right) \hat{y} \right] \quad (6)$$

for rectangular waveguide TM_{mn} modes, where ϵ_m is the Neumann factor and equals 1 for $m = 0$ and 2 for $m > 0$.

The periodicity of the infinite array simplifies the analysis to a study of a single equivalent element. If the problem did not have this periodicity, the mutual coupling would have to be evaluated element by element, increasing the complexity of the computation.

B. Boundary Conditions and Method of Moments

The electromagnetic field in the waveguide is expressed as a sum of incident and reflected waveguide modes, while in the free-space region it is expressed as a sum of incident and reflected Floquet modes. Boundary conditions are applied at the interface between two regions, i.e., the transverse electric and magnetic field must be continuous across the junction at $z = 0$. This leads to an integral equation for the unknown transverse electric field at the boundary. The infinite-array scattering problem then becomes similar to a two-region waveguide problem.

The method of moments is used to transform the integral equation into a matrix equation suitable for evaluation on a digital computer. Solving the set of linear equations gives the unknown mode coefficients in both regions. The time required for filling the matrix depends on the number of Floquet and waveguide modes used. The number of waveguide modes and Floquet modes used in the program can be increased by the user to ensure convergence of the solution [5,6].

C. Scattering Matrix and Reference Plane

The characteristics of the infinite array referenced to $z = 0$ are represented by a scattering matrix **S** which contains the transmission and reflection information for the free-space/waveguide junction.

$$\mathbf{S} = \begin{bmatrix} S_{11} & S_{12} \\ S_{21} & S_{22} \end{bmatrix} \tag{7}$$

where S_{11}, S_{12}, S_{21}, and S_{22} are matrices with 1 representing the free-space region and 2 the waveguide region. The size of matrix S_{11} is 2 by 2, S_{22} is n by n, S_{12} is 2 by n, S_{21} is n by 2, and n is the number of waveguide modes used. For an arbitrary set of incident waveguide modes contained in vector a_1 and incident TE_{00} and TM_{00} Floquet modes contained in vector a_2, the reflected mode vectors b_1 and b_2 are determined by the following set of equations.

$$b_1 = S_{11}a_1 + S_{12}a_2 \tag{8}$$

$$b_2 = S_{21}a_1 + S_{22}a_2 \tag{9}$$

Moving the reference plane in the waveguide region from $z = 0$ to $z = -t/2$, Fig. 2(b), where t is the thickness of the plate, the elements of the new scattering matrix $\mathbf{S}'$ become

$$S'_{11}(u,v) = S_{11}(u,v) \tag{10}$$

$$S'_{12}(u,v) = S_{12}(u,v) \exp\left(-j\gamma_v \frac{t}{2}\right) \tag{11}$$

$$S'_{21}(u,v) = S_{21}(u,v) \exp\left(-j\gamma_u \frac{t}{2}\right) \tag{12}$$

$$S'_{22}(u,v) = S_{22}(u,v) \exp\left[\left(-j\gamma_u \frac{t}{2}\right)\left(-j\gamma_v \frac{t}{2}\right)\right] \tag{13}$$

where γ_u and γ_v are the propagation constants of modes u and v.

D. Cascading and Finite Thickness

Scattering by a dichroic plate with finite thickness can be analyzed by considering two infinite-array problems. The space is divided into four regions: a free-space region (region I), two waveguide regions (regions II and III), and another free-space region (region IV), as shown in Fig. 3. The scattering matrix with reference to $z = -t/2$ for regions I and II is $\mathbf{S}'$, and the scattering matrix with reference to $z = -t/2$ for regions III and IV is $\mathbf{S}''$, which is the transpose matrix of $\mathbf{S}'$.

$$S''_{11} = S'_{22} \tag{14}$$

$$S''_{12} = S'_{21} \tag{15}$$

$$S''_{21} = S'_{12} \tag{16}$$

$$S''_{22} = S'_{11} \tag{17}$$

The scattering matrix $\mathbf{S}^T$ for the finite-thickness plate is determined by cascading these two matrices.

$$S^T_{11} = S'_{12}(I - S''_{11}S'_{22})^{-1}S''_{11}S'_{21} + S'_{11} \tag{18}$$

$$S^T_{12} = S'_{12}(I - S''_{11}S'_{22})^{-1}S''_{12} \tag{19}$$

$$S^T_{21} = S''_{21}(I - S'_{22}S''_{11})^{-1}S'_{21} \tag{20}$$

$$S^T_{22} = S''_{21}(I - S'_{22}S''_{11})^{-1}S'_{22}S''_{12} + S''_{22} \tag{21}$$

where I is a unitary matrix.

III. Verification of the Computer Code

The dichroic plate computer program was first checked against the available calculations for a thick dichroic plate with square holes at normal incidence [7]. The results showed good agreement. Next, a 13.25-by-15.5-in. metallic dichroic plate (Fig. 4) was fabricated to verify the computer code. The dimensions of the plate are H_x = 0.771 in., H_y = 0.757 in., D_x = 0.940 in., D_y = 0.940 in., Ω = 60.0 deg, and t = 1.411 in., with a tolerance of 0.001 in. Figure 5 shows the convergence of the solution at 8.3 GHz for TM polarization with respect to the number of waveguide modes used. Satisfactory convergence is achieved by using 40 waveguide modes. The amplitude and phase of the transmission and reflection coefficients from 8 to 9 GHz were computed with 40 waveguide modes for TE and TM polarizations (Figs. 6–9). Since the plate was built merely to verify the software, it was not optimized for any specific passband.

The configuration of the experiment is shown in Fig. 10. The reflection coefficients were measured from 8 to 9 GHz for θ = 30 deg and ϕ = 90 deg. The feed used was a 22-dB corrugated horn with a far-field phase center 3.125 in. inside the horn aperture. A lens was added to the horn aperture to bring the far-field phase center to 2.0 in. outside the horn aperture. Since the new phase center was closer to the dichroic plate, a smaller plate with less than −25-dB edge taper was used.

The experimental results and the calculation using 40 waveguide modes are shown in Figs. 11 and 12 for TE

and TM linear polarization, respectively. The curves are in excellent agreement except for frequencies higher than 8.6 GHz for TM polarization. This area of discrepancy can be explained by considering the effects of non-plane-wave incidence.

The analysis of the thick dichroic plate assumes that a linearly polarized plane wave is incident on an infinite dichroic plate at 30 deg. In the experiment, a corrugated horn was used. The field radiated contains plane wave components that are incident at angles other than 30 deg. This can result in grating-lobe problems at high frequencies, as can be seen in Fig. 12 for frequencies above 8.6 GHz.

IV. Conclusion

An analysis of a thick dichroic plate with rectangular holes has been presented. The good agreement between calculation and experimental data demonstrates the accuracy of the software. Further studies on the grating lobes due to non-plane-wave incidence are in progress and will provide a better understanding of the performance of the dichroic plate when illuminated by a corrugated horn.

Acknowledgments

The author would like to thank P. Stanton and H. Reilly for performing the measurements, D. Hoppe and R. Hodges for technical discussions, and L. Epp for correcting a coding error in the program.

References

[1] T. Y. Otoshi and M. M. Franco, "Dual Passband Dichroic Plate for X-Band," *TDA Progress Report 42-94*, vol. April–June 1988, Jet Propulsion Laboratory, Pasadena, California, pp. 110–134, August 15, 1988.

[2] N. Amitay, V. Galindo, and C. P. Wu, *Theory and Analysis of Phased Array Antennas*, New York: Wiley-Interscience, 1972.

[3] C. C. Chen, "Transmission Through a Conducting Screen Perforated Periodically with Apertures," *IEEE Trans. Microwave Theory Tech.*, vol. MTT-18, no. 9, pp. 627–623, September 1970.

[4] C. C. Chen, "Transmission of Microwaves Through Perforated Flat Plates of Finite Thickness," *IEEE Trans. Microwave Theory Tech.*, vol. MTT-21, no. 1, pp. 1–6, January 1973.

[5] S. W. Lee, W. R. Jones, and J. J. Campbell, "Convergence of Numerical Solutions of Iris-Type Discontinuity Problems," *IEEE Trans. Microwave Theory Tech.*, vol. MTT-19, no. 6, pp. 528–536, June 1971.

[6] R. Mittra, T. Itoh, and T. S. Li, "Analytical and Numerical Studies of the Relative Convergence Phenomenon Arising in the Solution of an Integral Equation by the Moment Method," *IEEE Trans. Microwave Theory Tech.*, vol. MTT-20, no. 2, pp. 96–104, February 1972.

[7] S. W. Lee, G. Zarrillo, and C. L. Law, "Simple Formulas for Transmission Through Periodic Metal Grids or Plates," *IEEE Trans. Antenna Propagat.*, vol. AP-30, no. 5, pp. 904–909, September 1982.

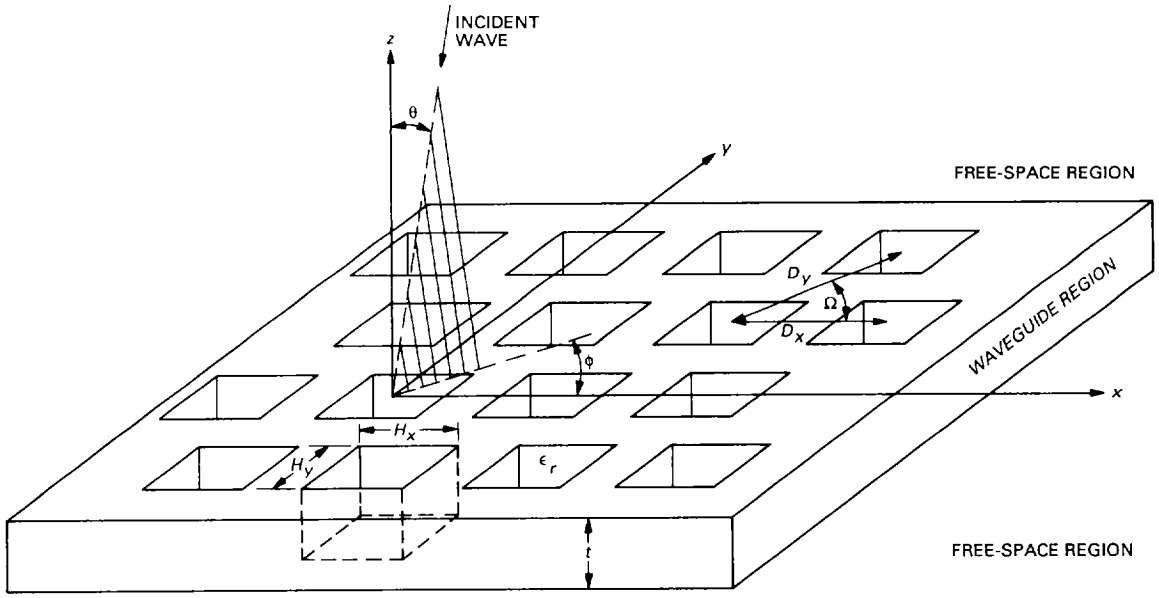

Fig. 1. Geometry of a thick dichroic plate with rectangular holes.

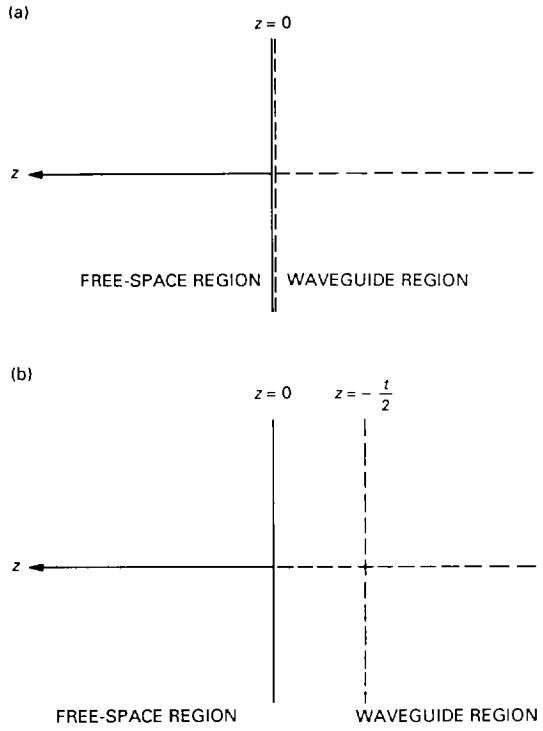

Fig. 2. Half-space infinite array with: (a) reference plane $z = 0$, and (b) reference plane $z = -t/2$.

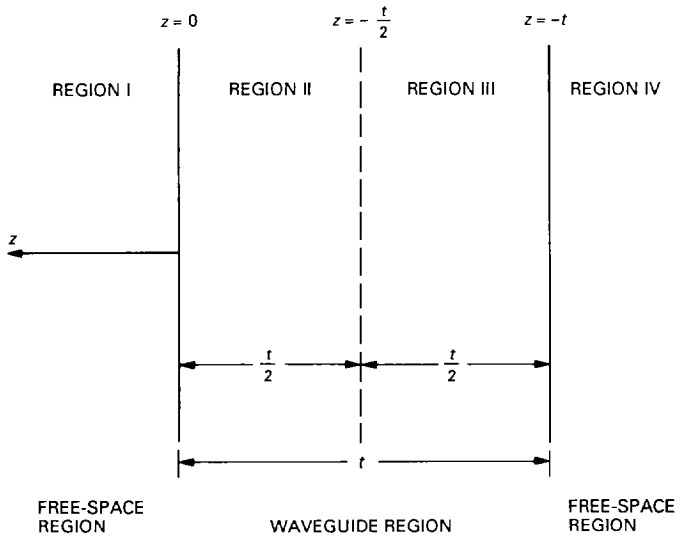

Fig. 3. Finite-thickness (t) plate is analyzed by considering two infinite-array problems.

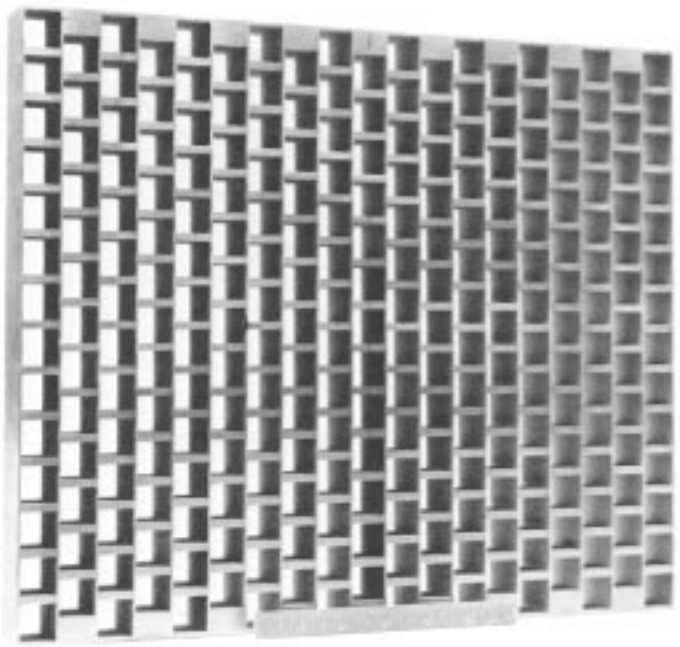

Fig. 4. Prototype dichroic plate.

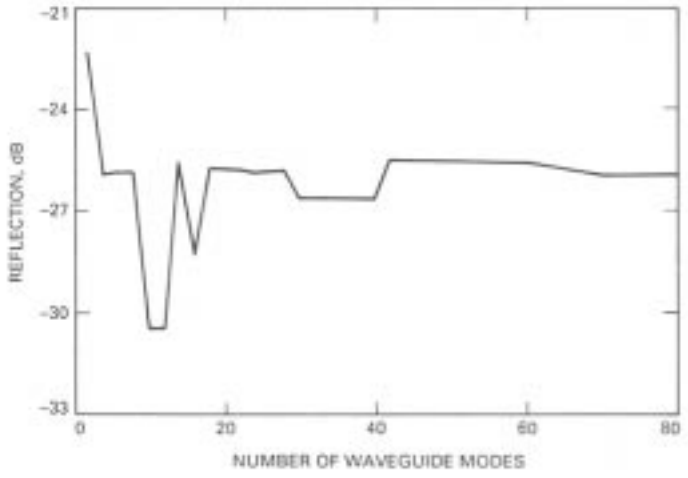

Fig. 5. Convergence with respect to the number of waveguide modes.

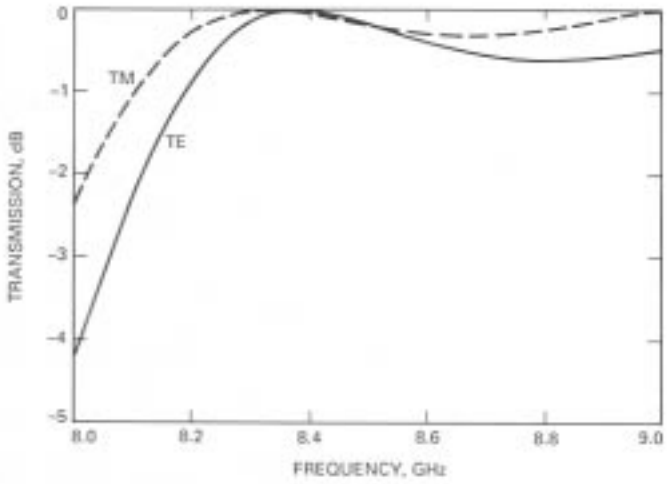

Fig. 6. Theoretical transmission versus frequency for the test dichroic plate for TE and TM polarization.

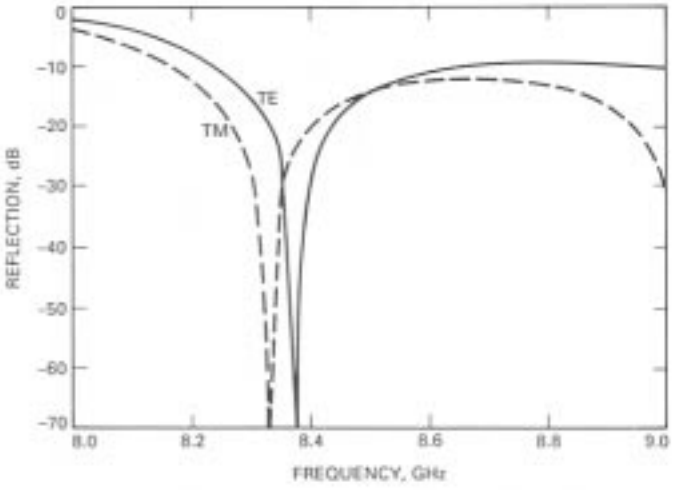

Fig. 7. Theoretical reflection versus frequency for the test dichroic plate for TE and TM polarization.

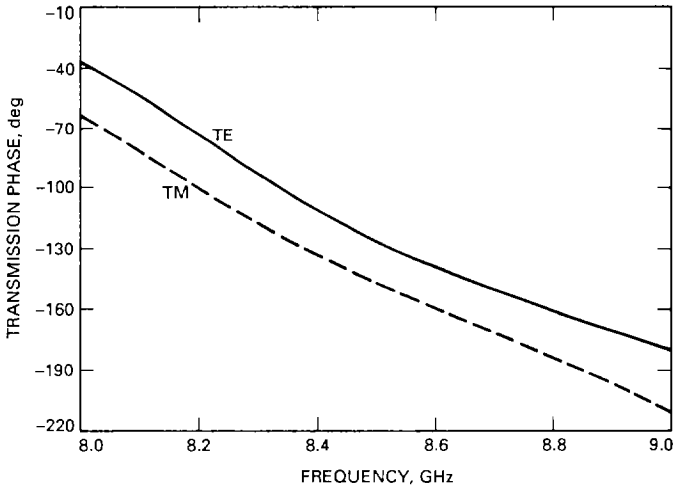

Fig. 8. Theoretical transmission phase versus frequency for the test dichroic plate for TE and TM polarization.

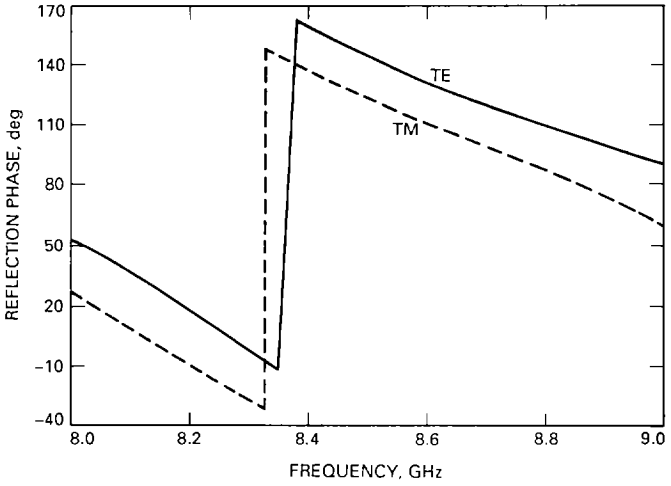

Fig. 9. Theoretical reflection phase versus frequency for the test dichroic plate for TE and TM polarization.

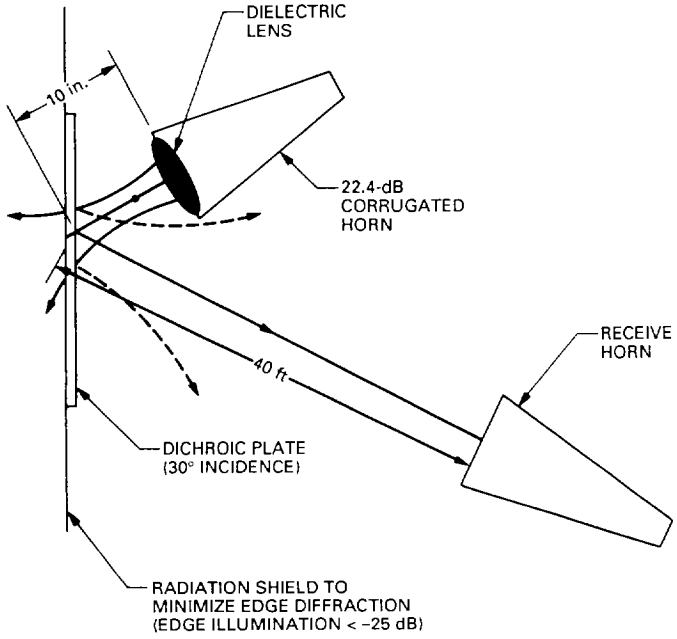

Fig. 10. Test setup for reflection measurements.

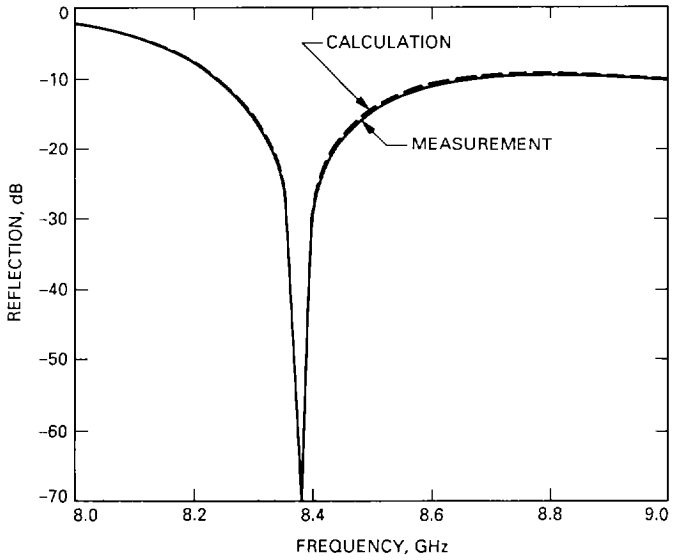

Fig. 11. Measured and calculated reflection versus frequency for the test dichroic plate for TE polarization.

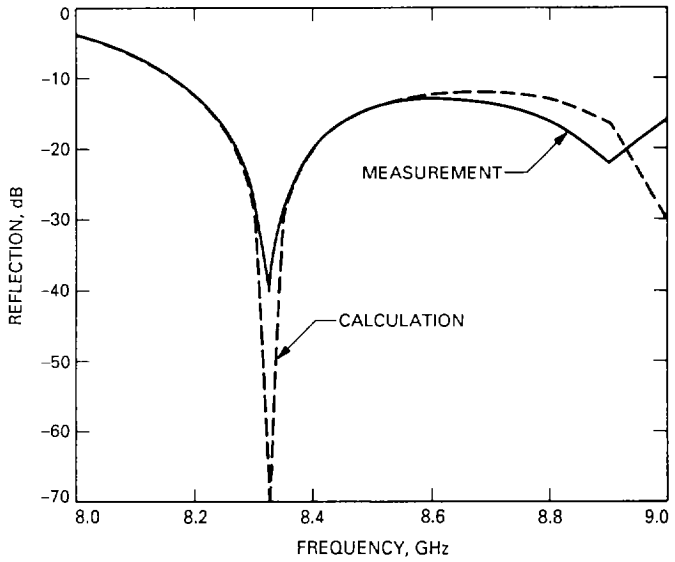

Fig. 12. Measured and calculated reflection versus frequency for the test dichroic plate for TM polarization.